Characterization and Application of Nanomaterials (2022) Volume 5 Issue 1
doi:10.24294/can.v5i1.1407

ORIGINAL RESEARCH ARTICLE

Study on the preparation and antibacterial properties of CTAB-coated AuNPs

Yayun Ma, Mei Liu*, Jiao Li, Xuanyi Li, Zongqi Yang

School of Food Engineering and Nutritional Science, Shaanxi Normal University, Xi'an 710119, China. E-mail: liumei@snnu.edu.cn

ABSTRACT

In this paper, spherical gold nanoparticles (AuNPs), rod-shape AuNPs and triangular AuNPs were synthesized using CTAB as the coating reagent, and their bactericidal properties against *Staphylococcus aureus* (*S. aureus*) and *Escherichia coli* (*E. coli*) were studied. By the plate count method and turbidity method, the minimum bactericidal concentrations (MBC) and the minimum bacteriostasis concentrations (MIC) to the two kinds of bacteria were determined. The MIC of rod-shape AuNPs, triangular AuNPs and spherical AuNPs to *E. coli* were 0.65 μg/mL, 3.71 μg/mL, 21.21 μg/mL, and MBC were 1.30 μg/mL, 11.09 μg/mL, 21.21 μg/mL, respectively. The MIC to *S. aureus* were 0.26 μg/mL, 0.56 μg/mL, 2.65 μg/mL, while MBC were 0.52 μg/mL, 1.11 μg/mL, 2.65 μg/mL, respectively. The results showed that the bactericidal effect of rod-shape AuNPs on *E. coli* and *S. aureus* was higher than that of the other two forms, and the bactericidal effect of three different forms of AuNPs on *S. aureus* was better than that on *E. coli*.

Keywords: AuNPs; Different Forms; *S. aureus*; *E. coli*; Antibacterial Properties

ARTICLE INFO

Received: 8 September 2021
Accepted: 21 October 2021
Available online: 5 November 2021

1. Introduction

Food safety issues have become a public health hotspot in today's world, while foodborne pathogenic bacteria are one of the main causes of foodborne diseases, and the emergence of antibiotics has played a big role in controlling such diseases. However, the abuse of antibiotics makes bacteria have gradually produced drug resistance to traditional antibiotics, and the emergence of antibiotic resistance pathogens has seriously jeopardized human health. Therefore, the research about new, safe, and efficient antibacterial materials is imminent[1].

In recent years, with the development of nanotechnology, the antibacterial study of nanomaterials has become a hot spot in current research. Antibacterial nanomaterials have been reported[2] including nanocrystallized traditional antibacterial materials (such as nanofibae, nanoplastic antimicrobial peptide, etc.), inorganic metals and metal oxide nanoparticles (such as gold, silver, copper, zinc oxide, etc.), and new surface modified nanoparticles. Nanoparticles are used as a new type of antibacterial drugs, which is considered to have a mechanism different from conventional drugs. It is difficult to induce bacterial resistance compared to traditional antibiotics. Therefore, it has become one of the novel drug research and development directions, attracting great interest of researchers[3,4].

AuNPs, highly representative nanoparticles, have a wide range of applications in the fields of catalytic[5], biomedicine[6] and other fields

with its good stability, dimensional effect, surface effect, optical effect, and unique biological affinity. In the field of biomedicine, "AuNPs" has become a favored nanomaterial, widely used in biological sensing[7–9], as drug delivery carriers[10,11], and as a new type of antibacterial drug after its surface is modified by different antibacterial drugs[3]. However, there is little study of AuNPs' self-antibacterial properties compared to that of the silver nanoparticles that are widely concerned.

In 2015, Z. Vivian Feng's topic group[12] obtained AuNPs with different charges by coating different agents on the surface and compared the antibacterial properties. They found that AuNPs with negative charges do not have bactericidal effect, while AuNPs with positive charges have bactericidal effect; with the increase of charge density, the bactericidal effect is constantly enhanced. In 2017, Jelle Penders's topic group[13] studied the effects of negative AuNPs, GNFs, gold nanostars on the lag time and exponential growth rate of *S. aureus* growth, and observed an obvious concentration and shape dependency effect. The change of shapes caused significant difference in the antibacterial effect. It is speculated that this is due to the large surface area and more surface protrusions, which may make GNFs more easily attached to the bacteria, then break the membrane, resulting in cell death.

Hexadalkyl trimethyl ammonium bromide (CTAB) is the most commonly used coating agent to synthesizing AuNPs with positive charges, and the CTAB coated method has been found to be able to synthesize AuNPs in many shapes such as rod, triangle, sphere, and cube[14], of which rod-shape AuNPs, spherical AuNPs, triangular AuNPs have better stability, a simpler synthetic method, and are applied in a wide range of fields. Based on this, we chose to use CTAB as a coating agent to study the antibacterial activity of positively charged AuNPs with spherical, rod-shape and triangular morphology.

In this paper, three kinds of positively charged AuNPs with spherical, rod-shape and triangular morphology were synthesized by using CTAB as the coating reagent, and *S. aureus* from gram-positive bacteria and *E. coli* from gram-negative bacteria were used as test strains. By the plate count method and turbidity method, we determined the minimum bactericidal concentrations and minimum antibacterial concentrations of the two bacteria, and studied the antibacterial effect of the three different forms of positively charged AuNPs on test strains. And the mechanism of antibacterial action is discussed.

2. Experiment

2.1 Reagents and instruments

Chlorogenic acid ($HauCl_4$), CTAB, silver nitrate ($AgNO_3$), sodium borohydride ($NaBH_4$), ascorbic acid (AA), trisodium citrate ($C_6H_9Na_3O_9$), isopropyl alcohol (C_3H_8O), anhydrous ethanol (C_2H_5OH), sodium chloride (NaCl), potassium iodide (KI), phosphate buffer solution (PBS), agar powder, cerebral flux culture medium (BHI), broth medium (LB). The above reagents are all commercially available analytical reagents, and the experimental water is ultrapure water. The *S. aureus* (CICC 10384) and *E. coli* (K12) for the experiment is purchased in China Center of Industrial Culture Collection.

LDZX–30KBS vertical pressure steam sterilizer, Shanghai SHENAN Medical Device Factory; YT–CJ–2D ultra-clean workbench, Beijing Yatai Kelong Instrument Technology Co., Ltd.; DH4000II electric heating incubator, Telles Instrument (Tianjin) Co., Ltd.; PB–10 Satorius Basic pH Meter, Sartorius Scientific Instruments (Beijing) Co., Ltd.; ZD–85A dual-function constant temperature air bath shaker, Youlian Instrument Research Institute, Jintan City, Jiangsu Province; HC–3018R high speed refrigerated centrifuge, Zhonghai Branch of KDCS Co., Ltd.; DF–101S collective temperature heating magnetic mixer, Gongyi Yuhua Instrument Co., Ltd.; UV–1800 UV-visible spectrometer, Japan Hitachi; JEM–2100 transmission electron microscope, Japan Jeol; Cannon 500D digital camera, Canon Co., Ltd.

2.2 Preparation of AuNPs

2.2.1 Preparation of spherical AuNPs

According to the literature[15], 20 mL $HAuCl_4$ (2.5×10^{-4} M) solution was stirred with 0.0015 g trisodium citrate to make the concentration of trisodium citrate 2.5×10^{-4} M. Then 0.6 mL $NaBH_4$ solution (0.1 M) with ice water was added, and the solution immediately turned pink and was stirred continuously to act as seed fluid. 6 g CTAB was added to 200 mL $HAuCl_4$ (2.5×10^{-4} M) solution to make the concentration of CTAB 0.08 M, then the solution was heated at 45 ℃ until it turned orange, and cooled to room temperature to be used as a growth solution for later use (note: if crystals form, slowly dissolve them at a mild temperature). Add 0.05 mL prepared Vc (0.1 M) into 9 mL growth solution, add 1 mL seed solution under intense agitation, continue stirring for 10 min, then add 0.05 mL Vc (0.1 M) into 9 mL growth solution, add 1 mL dark red solution under intense agitation, continue stirring for 10 min to turn them into brownish red. The spherical AuNPs with a particle size of 17 ± 2.5 nm can be obtained.

Post-treatment: undertake centrifugation at 10,000 r/min at 30 ℃ for 15 min, remove the supernatant, replenish water to 10 mL, repeat the centrifugation process twice, and finally dilute the sediment to half of its original volume with water, and store it under 4 ℃ away from light.

2.2.2 Preparation of rod-shape AuNPs

According to the method in the literature[16], 5 mL $HAuCl_4$ (5.0 mM) solution was added to 5 mL CTAB (0.2 M) solution and stirred, and the solution changed from bright yellow to orange. Continue stirring and add 0.6 mL $NaBH_4$ (0.01 M) solution (prepared when necessary), stir for 2 min, and the solution turned yellowish-brown. Finally, the AuNPs solution was heated at constant temperature for 2 h in a 30 ℃ water bath, and then used as seed liquid. In 5 mL CTAB (0.2 M) solution, 0.1 mL $AgNO_3$ (0.004 M) solution was added in the process of stirring, followed by 5 mL $HAuCl_4$ (1 mM) solution, and 70 mL AA (0.0788 M) solution. After the solution became colorless, add 12 μL crystal seed. Continue stirring for 15 min, and the solution turned purple. Finally, the solution of AuNPs was heated in a 30 ℃ water bath for 2 h at constant temperature. The solution turned dark blue and the rod-shape AuNPs could be obtained. The post-treatment process is the same as that of spherical AuNPs.

2.2.3 Preparation of triangular AuNPs

According to the literature[17], 0.4 mL $HAuCl_4$ (2.5×10^{-4} M) and 1 mL sodium citrate (10 mM) were added to 37.6 mL water, followed by 1 mL $NaBH_4$ solution with ice water (0.1 M). After vigorously stirring for 2 min, the solution turned orange-red, and then stood for 2 h to ensure that the unreacted $NaBH_4$ was completely hydrolyzed to make seed liquid. 100 mL growth solution containing 2.5×10^{-4} M $HAuCl_4$ solution and 0.05 M CTAB was added with 55 μL KI (0.1 M), 0.55 mL Vc (0.1 M), and 0.55 mL NaOH (0.1 M), stirred gently until the solution turned orange, then cooled to room temperature as a growth solution for later use. 0.1 mL seed liquid was added to the growth solution, and the color of the growth solution changed from transparent to light red, and then to deep red within 30 min (the reaction solution was kept at 30 ℃), then triangular AuNPs were obtained. The post-treatment process is the same as that of spherical AuNPs.

2.3 Characterization of samples

A UV–1800 UV-visible spectrometer (UV-VIS, Japan's compnay) was used to record the UV spectrum of the samples for quickly distinguishing spherical AuNPs, rod-shape AuNPs and triangular AuNPs. The morphology and particle size of the three different AuNPs were observed by TEM (Jeol, Japan).

2.4 Test of antibacterial performance

The minimum bactericidal concentration (MBC) and minimum inhibitory concentration (MIC) to *E. coli* and *S. aureus* were detected by the plate count method and 96-well plate method.

2.4.1 Preparation of medium

Take 37 g brain heart infusion and culture it in 1 L distilled water, boil it to make it fully dissolved,

adjust pH to 7.2–7.3, add 15 g AGAR powder (AGAR powder is not needed if liquid medium is prepared). After boiling and dissolving, sterilize it at 121 ℃ for 20 min, and pour it to the plate on an aseptic operating table for later use.

Broth medium was prepared by the same method.

2.4.2 Preparation of bacterial suspension

The bacteria cryopreservation tube was taken out from the refrigerator at 80 ℃. After the solution was dissolved, the bacteria solution was diluted to 10^{-2}, 10^{-4}, 10^{-6} times by the two-fold dilution method[18,19]. 100 μL of each was applied to the plate and cultured at 37 ℃ for 18 h. Take out 20 mL sterilized liquid medium and transfer it to a 100 mL conical flask, then use a 10 μL pipetting gun to absorb a complete colony. Put the spear tip into the conical flask and incubate it on a shaker (37 ℃, 260 r/min) for 14 h. Centrifuge (6,000 r/min, 2 min) for removing the supernatant, add 5 mL normal saline, mix well and centrifuge (6,000 r/min, 2 min), repeat twice, then add 5 mL normal saline to the bacteria removed from the medium, mix evenly and set aside for use.

2.4.3 Minimum bactericidal concentration

Add AuNPs diluted to different concentrations to PBS buffer solution, then add 100 μL of bacterial solution with a dilution ratio of 2×10^4 and mix them to make the reaction system 1,000 μL. After incubation in a shaker for 4 h, take out 100 μL and spread it on the culture plate, culture upside down at 37 ℃ for 18 h, and observe the colony growth. The mixture of PBS buffer solution and bacteria solution was used as the blank control. Three parallel experiments were performed. The colony growth was observed, and the concentration corresponding to the sample with less than 5 colonies was taken as the MBC value.

2.4.4 Minimum inhibitory concentration

Add AuNPs diluted to different concentrations into the liquid medium, and then add 100 μL bacterial solution with a dilution ratio of 2×10^4 to make the reaction system 1,000 μL. Add 200 μL to the area of 96-well plate as the experimental group; the AuNPs solution in the experimental group was replaced with the same amount of normal saline, and then 200 μL was added to the corresponding area of the 96-well plate as the positive control. Change the bacteria liquid and liquid medium of the experimental group into the same amount of normal saline, and add 200 μL to the 96-well plate area as the negative control. The 96-well plate was placed in a constant temperature incubator and incubated at 37 ℃ for 24 h. The MIC was the concentration of AuNPs that could prevent the sample from forming obvious turbidity.

3. Results and discussion

3.1 Characterization of AuNPs

3.1.1 UV-visible absorption spectrum analysis

Figure 1 shows the results of UV-absorbable spectrum analysis after the synthesis of AuNPs. UV spectrum analysis shows that: absorption peaks of spherical AuNPs were at 520 nm, that of rod-shape AuNPs were at 525 nm and 604 nm, and that of triangular AuNPs were at 728 nm and 928 nm, which were basically consistent with the absorption peaks in the references, confirming the successful synthesis of spherical AuNPs, rod-shape AuNPs and triangular AuNPs.

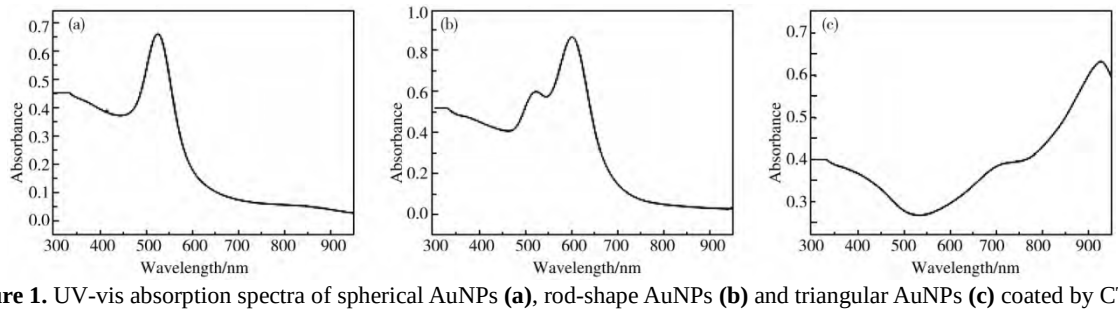

Figure 1. UV-vis absorption spectra of spherical AuNPs **(a)**, rod-shape AuNPs **(b)** and triangular AuNPs **(c)** coated by CTAB.

3.1.2 Transmission electron microscopy (TEM)

Through TEM, three different forms and particle sizes of the synthesized AuNPs can be intuitively observed, as shown in **Figure 2**. It can be seen from the figure that the three different forms of AuNPs were successfully prepared, and were relatively uniform with good dispersion among the particles. The diameter of the spherical AuNPs is about 17 ± 2.5 nm, the length of the rod-shape AuNPs is about 52.31 ± 0.86 nm, with the width about 22.49 ± 0.56 nm and the aspect ratio about 2.3. The synthesized triangular AuNPs are equilateral with the side length of 100 ± 25 nm.

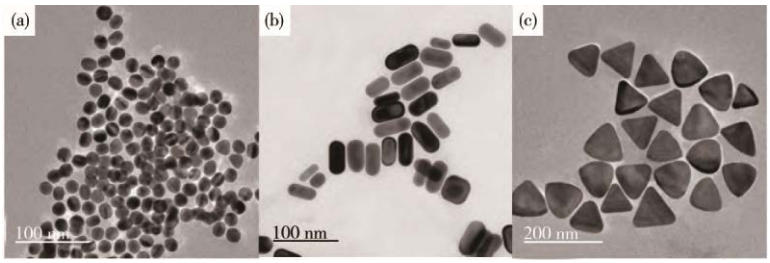

Figure 2. TEM images of spherical AuNPs **(a)**, rod-shape AuNPs **(b)** and triangular AuNPs **(c)** coated by CTAB.

3.2 Study on bactericidal effect of different forms of AuNPs

3.2.1 Minimum bactericidal concentration of spherical AuNPs

As shown in **Figure 3**, the MBC of spherical AuNPs to *E. coli*: when the concentration of AuNPs is greater than 21.21 μg/mL, the number of bacterial colonies on the plate is less than 5, so the MBC is 21.21 μg/mL; for the MBC to *S. aureus*: when the concentration of AuNPs is greater than 5.30 μg/mL, the number of bacterial colonies on the plate is less than 5, so the MBC of spherical AuNPs is 5.30 μg/mL.

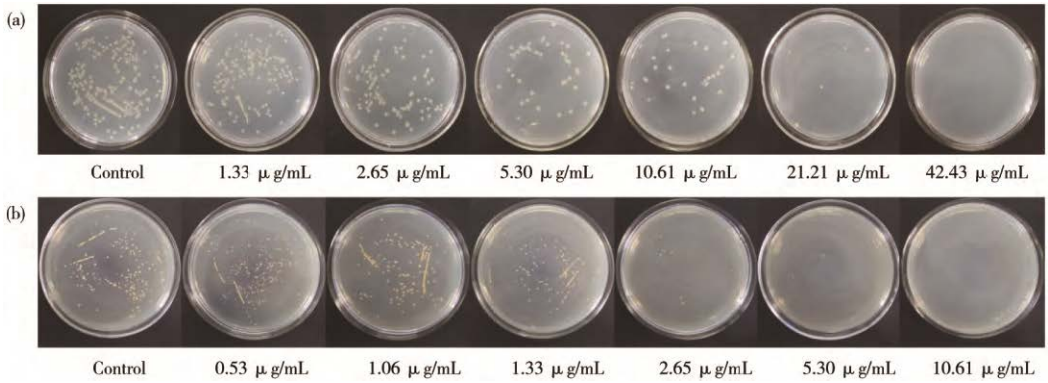

Figure 3. Plate diagram of *E. coli* **(a)** and *S. aureus* **(b)** under different concentrations of spherical AuNPs.
Note: AuNPs reacted with bacterial solution for 4 h, and the plate was cultured at 37 ℃ for 18 h.

3.2.2 Minimum bactericidal concentration of rod-shape AuNPs

As can be seen from **Figure 4**, when the concentration of rod-shape AuNPs was greater than 1.30 μg/mL, the number of bacterial colonies on the plate was less than 5, so the MBC to *E. coli* was 1.30 μg/mL. When the concentration of AuNPs was greater than 0.52 μg/mL, the number of bacterial colonies on the plate was less than 5, and the MBC to *S. aureus* was 0.52 μg/mL.

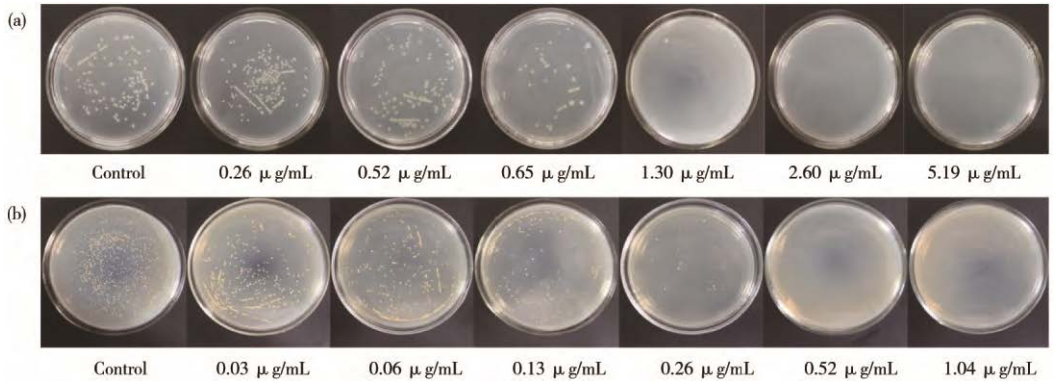

Figure 4. Plate diagram of *E. coli* **(a)** and *S. aureus* **(b)** under different concentrations of rod-shape AuNPs.
Note: AuNPs reacted with bacterial solution for 4 h, and the plate was cultured at 37 ℃ for 18 h.

3.2.3 Minimum bactericidal concentration of triangular AuNPs

As can be seen from **Figure 5**, when the concentration of AuNPs is greater than 11.09 μg/mL, the number of bacterial colonies on the plate is less than 5, so the MBC to *E. coli* is 11.09 μg/mL. For the MBC to *S. aureus*, when the concentration of AuNPs is greater than 1.11 μg/mL, the number of bacterial colonies on the plate is less than 5, so the MBC of triangular AuNPs is 1.11 μg/mL.

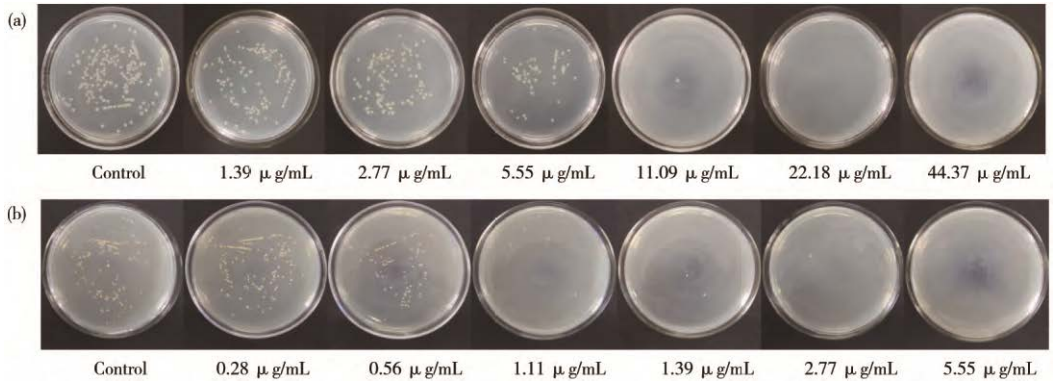

Figure 5. Plate diagram of *E. coli* **(a)** and *S. aureus* **(b)** under different concentrations of triangular AuNPs.
Note: AuNPs reacted with bacterial solution for 4 h, and the plate was incubated at 37 ℃ for 18 h.

3.3 Study on inhibitory effects of different forms of AuNPs

3.3.1 *Staphylococcus aureus*

Taking *S. aureus* as the research object, the different forms of synthesized AuNPs were diluted, respectively, the dilution ratio of spherical AuNPs was 10, 20, 40, 80, 160 times, and that of rod-shape AuNPs was 1,000, 2,000, 4,000, 8,000, 10,000 times, and that of triangular AuNPs was 50, 100, 200, 400 and 800 times. The concentration of AuNPs corresponding to the dilution ratio was used to determine the minimum inhibitory concentration, and the results of the 96-well plate were shown in **Figure 6**. The results showed that the MIC of spherical AuNPs to *S. aureus* was 2.65 μg/mL, that of rod-shpe AuNPs was 0.26 μg/mL, and that of triangular AuNPs was 0.56 μg/mL.

Figure 6. The MIC of spherical AuNPs **(a)**, rod-shape AuNPs **(b)** and triangular AuNPs **(c)** coated by CTAB to *S. aureus* cultured at 37 ℃ for 24 h.
Note: The figure is the concentration of AuNPs, in μg/mL.

3.3.2 *Escherichia coli*

E. coli was taken as the research object, and the different forms of AuNPs were diluted. Respectively, the dilution ratios of spherical AuNPs were 5, 10, 20, 40, 80 times, that of rod-like AuNPs were 400, 800, 1,000, 2,000, 4,000 times, and that of triangular AuNPs were 30, 60, 120, 240, 800 and 480 times. The MIC of AuNPs of different forms was determined at the concentration corresponding to different dilution ratios, and the results of 96-well plates were shown in **Figure 7**. The results showed that to *E. coli*, the MIC of spherical AuNPs was 21.21 μg/mL, that of rod-shape AuNPs was 0.65 μg/mL, and that of triangular AuNPs was 3.70 μg/mL.

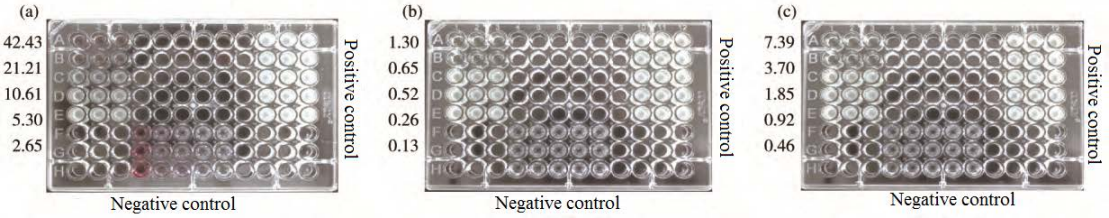

Figure 7. The MIC of spherical AuNPs **(a)**, rod-shape AuNPs **(b)** and triangular AuNPs **(c)** coated by CTAB to *E. coli* cultured for 24 h at 37 ℃.
Note: The figure is the concentration of AuNPs, in μg/mL.

In conclusion, the MBC and MIC of AuNPs with different forms to *S. aureus* and *E. coli* were determined by the plate counting method and 96-well plate method, as shown in **Table 1** below. The bactericidal effect of rod-shape AuNPs is the best among the three forms of AuNPs. And no matter what form of AuNPs, its bactericidal effect on *S. aureus* is obviously better than that on *E. coli*.

Table 1. MIC and MBC of AuNPs with different forms

	MBC /μg·mL^{-1}		**MIC /μg·mL^{-1}**	
	E. coli	*S. aureus*	*E. coli*	*S. aureus*
Spherical AuNPs	21.21	5.30	21.21	2.65
Rod-shape AuNPs	1.30	0.52	0.65	0.26
Triangular AuNPs	11.09	1.11	3.70	0.56

3.4 Discussion on antibacterial mechanism

In 2014, Xingyu Jiang's research group[20] studied the bactericidal mechanism of AuNPs against gram-negative bacteria *E. coli* by means of transcription and proteomics, and found that there are two ways of action: one is to inhibit the activity of ATPase and reduce the level of ATP by destroying the membrane potential of bacterial cell membrane. The other is to inhibit ribosomal subunit binding to transport RNA. It was found that although ROS generation is the main reason for the bactericidal effect of most antibiotics and antibacterial nanomaterials, the antibacterial activity of AuNPs does not induce any related processes.

Zhang *et al.*[21] used polyethylene imine and bovine serum protein modified AuNPs and AuNPs rod as gene carriers, and found that the tip of rod-shape AuNPs had large curvature, resulting in higher charge density than spherical AuNPs. Moreover, most of the rod-shape particles will contact the cell membrane through the tip, leading to higher gene transfection efficiency when using rod-shape particles as the gene carrier. Due to its special form, rod-shape AuNPs have advantages in contacting with bacteria. In our experimental results, the bactericidal effect of rod-shape AuNPs is better than that of the other two forms of AuNPs, which may be due to this special contact mode.

The surface charge of nanoparticles plays an obvious role in their antibacterial ability[22]. For example, Angelique's team[23] studied the effects of different particle diameters and Zeta potential on the bactericidal activity of titanium dioxide nanoparticles, and found that titanium dioxide nanoparticles with about the same diameter showed stronger antibacterial effect when Zeta potential was higher. This indicates that the enhancement of surface charge is also a way to enhance the bactericidal effect, and the negatively charged nanoparticles will have a certain repulsion effect on negatively charged bacteria[24,25].

We conducted Zeta potential to verify the relationship between the bactericidal effect and charge density of different forms of AuNPs in this experi-

ment. The Zeta potential of rod-shape AuNPs was 56.8 mV, that of spherical AuNPs was 42.1 mV, and that of triangular AuNPs was 33.2 mV. As shown in **Figure 8**, three forms of AuNPs really are positively charged, and rod-shape AuNPs are with higher charge density compared with other two forms of AuNPs. At the same time, our experimental results show that compared with other two forms, rod-shape AuNPs have better bactericidal effect, which further illustrates that AuNPs with positive charges on the surface will see an enhanced bactericidal effect with the increase of charge density.

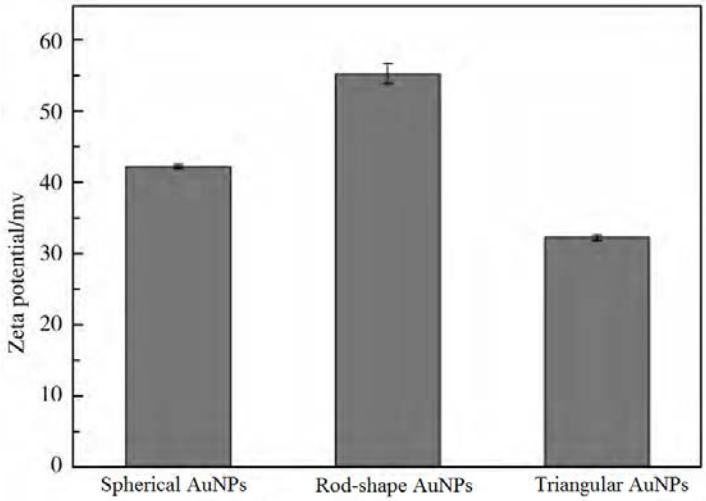

Figure 8. Zeta potentials of spherical AuNPs, rod-shape AuNPs and triangular AuNPs coated by CTAB.

4. Conclusion

CTAB-coated AuNPs of different forms (spherical, rod-shape, triangle) were prepared and *S. aureus* and *E. coli* were used as test strains. It can be seen in the study of antibacterial properties, no matter against *S. aureus* and *E. coli*, and the bactericidal effect of rod-shape AuNPs is higher than the other two forms of AuNPs. The surface of bacteria is with negative charges, and positively charged nanoparticles are attracted by bacteria with negative charge on the surface, contacting and destroying the cell membrane of bacteria to enter and kill bacteria. Rod-shape AuNPs are easier to contact bacteria from spatial effects, which is why they have a higher bactericidal property. The three forms of AuNPs are demonstrated to have better bactericidal effect against *S. aureus* than that against *E. coli*, which may be due to the different cell walls of the two bacteria. All these results laid the foundation for further work.

Conflict of interest

The authors declare that they have no conflict of interest.

Acknowledgements

Project of Central University Basic Research Business Fund (GK201802012); Shaanxi Science and Technology Plan Project (2017NY-121).

References

1. Dizaj SM, Lotfipour F, Barzegar-Jalali M, *et al*. Antimicrobial activity of the metals and metal oxide nanoparticle. Materials Science and Engineering: C 2014; 44: 278–284.
2. Ma W, Cui Y, Zhao Y, *et al*. Progress of antibacterial mechanisms study on nanoparticles. Acta Biophysica Sinica 2010; 26(8): 638–648.
3. Zhao Y, Tian Y, Cui Y, *et al*. Small molecule-capped gold nanoparticles as potent antibacterial agents that target gram-negative bacteria. Journal of the American Chemical Society 2010; 132(35): 12349–12356.
4. Li Y, Chen X. Preparation and mechanism of graphene-Ag antibacterial materials. Journal of Liaocheng University (Natural Science Edition) 2014; 27(3): 71–74.
5. Corma A, Garcia H. Supported gold nanoparticles as catalysts for organic reactions. Chemical Society

Reviews 2008; 37: 2096–2126.
6. Prabaharan M, Grailer JJ, Pilla S, *et al*. Gold nanoparticles with a monolayer of doxorubicin-conjugated amphiphilic block copolymer for tumor-targeted drug delivery. Biomaterials 2009; 30(30): 6065–6075.
7. Yáñez-Sedeño P, Pingarrón JM. Gold nanoparticle-based electrochemical biosensors. Analytical and Bioanalytical Chemistry 2005; 382(4): 884–886.
8. Lin YW, Huang CC, Chang HT. Gold nanoparticle probes for the detection of mercury, lead and copper ions. Analyst 2011; 136(5): 863–871.
9. Guo Y, Wang Z, Qu W, *et al*. Colorimetric detection of mercury, lead and copper ions simultaneously using protein-functionalized gold nanoparticles. Biosensors and Bioelectronics 2011; 10(15): 4064–4069.
10. Gu H, Ho PL, Tong E, *et al*. Presenting vancomycin on nanoparticles to enhance antimicrobial activities. Nano Letters 2003; 3(9): 1261–1263.
11. Tom RT, Suryanarayanan V, Reddy PG, *et al*. Ciprofloxacin-protected gold nanoparticles. Langmuir 2004; 20(5): 1909–1914.
12. Pal S, Tak YK, Song JM. Does the antibacterial activity of silver nanoparticles depend on the shape of the nanoparticle? A study of the Gram-negative bacterium *Escherichia coli*. Applied and Environmental Microbiology 2020; 73(6): 1712–1720.
13. Penders J, Stolzoff M, Hickey DJ, *et al*. Shape-dependent antibacterial effects of non-cytotoxic gold nanoparticles. International Journal of Nanomedicine 2017; 12: 2457–2468.
14. Yang X, Yang M, Pang B, *et al*. Gold nanomaterials at work in biomedicine. Chemical Reviews 2015; 115(19): 10410–10488.
15. Jana NR, Gearheart L, Murphy CJ. Seeding growth for size control of 5−40 nm diameter gold nanoparticles. Langmuir 2001; 17(22): 6782–6786.
16. Wang Y, Zhou X, Xu C, *et al*. Gold nanorods as visual sensing platform for chiral recognition with naked eyes. Scientific Reports 2018; 8(1): 5296–5304.
17. Guo Z, Fan X, Liu L, *et al*. Achieving high-purity colloidal gold nanoprisms and their application as biosensing platforms. Journal of Colloid and Interface Science 2010; 348(1): 29–36.
18. Fang M, Chen J, Xu X, *et al*. Antibacterial activities of inorganic agents on six bacteria associated with oral infections by two susceptibility tests. International Journal of Antimicrobial Agents 2006; 27(6): 513–517.
19. Kim J, Marshall MR, Wei CI. Antibacterial activity of some essential oil components against five foodborne pathogens. Journal of Agricultural and Food Chemistry 1995; 43(11): 2839–2845.
20. Cui Y, Zhao Y, Tian Y, *et al*. The molecular mechanism of action of bactericidal gold nanoparticles on *Escherichia coli*. Biomaterials 2012; 33(7): 2327–2333.
21. Zhang P, Li B, Du J, *et al*. Gold nanoparticles coated by polyethylenimine-g-bovine serum albumin with different morphologies for effective gene delivery. Journal of Controlled Release 2017; 259: e102–e103.
22. Seil JT, Webster TJ. Antimicrobial applications of nanotechnology: Methods and literature. International Journal of Nanomedicine 2012; 7(1): 2767–2781.
23. Simon-Deckers A, Loo S, Mayne-L'hermite M, *et al*. Size-, composition- and shape-dependent toxicological impact of metal oxide nanoparticles and carbon nanotubes toward bacteria. Environmental Science & Technology 2009; 43(21): 8423–8429.
24. Silhavy TJ, Kahne D, Walker S. The bacterial cell envelope. Cold Spring Harbor Perspectives in Biology 2010; 2(5): a000414.
25. Dickson JS, Koohmaraie M. Cell surface charge characteristics and their relationship to bacterial attachment to meat surfaces. Applied and Environmental Microbiology 1989; 55(4): 832–836.